Three biofilm types produced by a model pseudomonad are differentiated by structural characteristics and fitness advantage

Anna Koza
Robyn Jerdan
Scott Cameron
Andrew J. Spiers

Revised Manuscript with additions shown in Blue

Three biofilm-types produced by a model pseudomonad are differentiated by structural characteristics and fitness advantage

Anna Koza, Robyn Jerdan, Scott Cameron & Andrew J. Spiers

Affiliation: School of Applied Sciences, Abertay University, Bell Street, Dundee DD1 1HG, UK.

Author for correspondence: Andrew J. Spiers. Email: a.spiers@abertay.ac.uk.

Keywords: Adaptive radiation, air-liquid (A-L) interface biofilms, competitive fitness, experimental evolution, microcosms, *Pseudomonas, P. fluorescens* SBW25, Wrinkly Spreader.

Abbreviations: A-L Interface, Air-liquid interface; CBFS, Complementary Biofilm–Forming Strain; VM, Viscous Mass; WS, Wrinkly Spreader.

ABSTRACT

(249 words) Model bacterial biofilm systems suggest that bacteria produce one type of biofilm which is then modified by environmental and physiological factors, though diversification of developing populations might result in the appearance of adaptive mutants producing altered structures with improved fitness advantage. Here we compare the air-liquid interface Viscous Mass (VM) biofilm produced by *Pseudomonas fluorescens* SBW25 and the Wrinkly Spreader (WS) and Complementary Biofilm-forming Strain (CBFS) biofilm-types produced by adaptive SBW25 mutants in order to better understand the link between these physical structures and the fitness advantage they provide in experimental microcosms. Wrinkly Spreader, CBFS and VM biofilms can be differentiated by strength, attachment levels and rheology, as well as by strain characteristics associated with biofilm–formation. Competitive fitness assays demonstrate that they provide similar advantage under static growth conditions but respond differently to increasing levels of physical disturbance. Pairwise competitions between biofilms suggest that these strains must be competing for at least two growth-limiting resources at the air-liquid interface, most probably O_2 and nutrients, though VM and CBFS cells located lower down in the liquid column might provide an additional fitness advantage through the colonisation of a less competitive zone below the biofilm. Our comparison of different SBW25 biofilm-types illustrates more generally how varied biofilm characteristics and fitness advantage could become among adaptive mutants arising from an ancestral biofilm–forming strain and raises the question of how significant these changes might be in a range of medical, biotechnological and industrial contexts where diversification and change may be problematic.

INTRODUCTION

Biofilms are a form of surface–associated microbial aggregation which are significant in both natural and engineered environments, impacting on colonisation and infection, competitor, predator and host interactions, community dynamics and function, *etc.* (reviewed by [1-3]). It is easy to get the impression that there is a simple dichotomy between free-living and biofilm life-styles for most bacteria, but adaptive radiation within developing biofilm populations is likely to lead to diversification unless maintained by stabilizing selection [3]. As a result, it is interesting to ask whether bacteria produce a single biofilm-type based on a linear genetic architecture involving a single sensory-regulatory system controlling one biofilm matrix or extracellular polymeric substance (EPS) biosynthesis pathway, or whether they can produce a range of different structures which better suit the environmental based on a more complex networked architecture involving multiple regulatory and biosynthesis pathways and

modified by adaptive mutation. This can be explored using the *Pseudomonas fluorescens* SBW25 model system in which adaptive radiation has produced a number of biofilm-types and success can be evaluated in the context of competing lineages in resource (O_2)-restricted environments (reviewed by [4,5]).

In the SBW25 model system, the wild-type colonists of static microcosms rapidly modify their environment and differentiates the liquid column into a high–O_2 region at the top of the liquid column and an O_2-depleted zone below [6] (this division is arbitrary; as growth continues and O_2 demand increases, the high–O_2 region becomes shallower and the O_2 flux deeper into the liquid column is reduced). As growth in these microcosms becomes increasingly O_2-limited, the high–O_2 region represents an ecological opportunity [7] for any adaptive lineage capable of colonising it, as cells located here are capable of faster growth, higher final population numbers and a fitness advantage over other competitors located lower down in the liquid column (the high–O_2 region, which includes the A-L interface, is also referred to as the Goldilocks zone of optimal growth [8,9]; see **Supplementary Figure S1** for a schematic showing these regions and zones in static microcosms).

Adaptive lineages arise in developing or diversifying populations with key innovations that allow them to interact with their environment in a novel manner [7]. In diversifying SBW25 populations, Wrinkly Spreader (WS) mutants [10] occur with mutations affecting cyclic diguanylate (c-*di*-GMP) homeostasis and the over-production of cellulose which is the primary biofilm matrix (EPS) and a second poly-acetyl glucosamine EPS which may also acting as an attachment factor [11-15]. This results in the formation of a robust and well-attached physically cohesive-class biofilm [16] at the air-liquid (A-L) interface of static microcosms [10]. In contrast, wild-type SBW25, which does not form a biofilm under normal conditions (but see [17]), relies instead on constant aerotaxis to oppose physical disturbance and random cell diffusion, which constantly moves cells away from the high-O_2 region [9]. This, however, is not as effective as biofilm-formation in terms of resource utilisation and growth gains and explains why Wrinkly Spreaders often have fitness advantages over non-biofilm–forming competitors in static microcosms [10,12,18]. The underlying basis of this might be a trade-off between the use of uridine-triphosphate (UTP) for fast growth (DNA/RNA and metabolism) and the formation of uridine-diphosphate glucose (UDP-glucose) which is the precursor for cellulose [19] that enables biofilm-formation (after [20]).

A-L biofilm–formation is commonplace amongst environmental pseudomonads [21-25] and other bacteria, suggesting that many aerobic bacteria can gain a competitive advantage by growing in the high–O_2 region of static microcosms if growth is not limited by some other resource, and in several

model systems, including *Bacillus subtilis* 3610 [26], *P. aeruginosa* PA01 and PA14 [27,28], *P. putida* KT2440 [29] and SBW25, wild-type strains are known to produce multiple mutants with different biofilm characteristics. In addition to the Wrinkly Spreader, SBW25 produces a range of other physically cohesive-class biofilm-forming lineages with similar fitness advantage. These include the Fuzzy Spreaders evolved from wild-type SBW25 [10] which produce biofilms as the result of changes in lipopolysaccharide expression [30], and Poly-acetyl glucosamine-Wrinkly Spreader (PWS) and Complementary Biofilm-forming Strain (CBFS) mutants that evolved from a cellulose-deficient SBW25 strain and over-produce poly-acetyl glucosamine [15,31]. Wild-type SBW25 can also produce a cellulose-based but fragile and poorly-attached viscous mass-class biofilm (VM) [16] when induced with exogenous Fe^{3+} [17,32], similar to that produced by a genetically-engineered mutant using a strong promoter to over-express the cellulose biosynthesis operon [11,13]. Although these lineages arose independently from the wild-type SBW25 strain or other intermediates, they can be considered to have convergently evolved and adapted to the A-L interface of static microcosms with similar biofilms.

We are interested in comparing SBW25 biofilm-types, in particular the CBFS, VM and WS biofilms (see **Table 1** for key strain details including biofilm characteristics), in order to understand the link between environmental conditions, physical structure and the fitness advantage they provide. In this work, we induce wild-type SBW25 to produce VM biofilms and use a CBFS mutant as proxies for naturally-occurring SBW25 mutants which produce biofilms with similar physical characteristics and fitness advantage, and use biofilm strength and attachment measurements, rheology and other assays to quantitatively differentiate these structures and strains. We then compare CBFS, VM and WS biofilms using competitive fitness assays to determine how well suited they are to static microcosms and whether one biofilm-type is likely to be a more successful solution to the problem of colonising the A-L interface than the others.

MATERIALS AND METHODS

Experimental microcosms, bacteria and culturing

Biofilm-formation and fitness were investigated using wild-type *Pseudomonas fluorescens* SBW25 [33,34] that produces the VM biofilm (to avoid confusion we refer to this as the 'VM strain' throughout), a CBFS mutant [31] and the archetypal Wrinkly Spreader (WS) mutant [11,14] (**Table 1**). SM-13 (SBW25 *wssB*::mini-*Tn*5, selected with 50 μg ml^{-1} kanamycin [11]), was used as a non-biofilm–forming reference strain when required. Microcosms were 30 ml universal glass vials containing 6 ml King's B liquid medium supplemented with 1 μM $FeCl_3$ required to induce the VM biofilm (KB-Fe [17]) and preliminary

experiments had shown that the growth and phenotypes of CBFS and WS were the same in KB-Fe as they had been reported for in KB. Inocula were obtained from shaken over-night KB-Fe cultures, and microcosms were incubated at 18-20°C statically or with increasing levels of physical disturbance provided by a Stuart SSM1 shaker operating at 30 (low level of disturbance) and 80 rpm (intermediate), and a Stuart S150 incubator operating at 150 rpm (high, i.e. vigorous shaking).

Biofilm measurements and rheometry

Biofilms were qualitatively assessed by visual inspection *in situ* and after transferring to Petri dishes [16]. Biofilm strength and attachment to the vial walls at the meniscus of static microcosms after 48 h were determined using glass balls (strength, g; n = 8) and Crystal violet staining (attachment, A_{570}; n = 8) [12,21]. Rheological parameters (G', G", G*, η_0, and tan δ; n = 10 - 17) of biofilm samples were measured by controlled-stress amplitude sweep tests using a MARS rotational rheometer (Thermo Scientific, UK). Measurements were made at 20 ± 0.1 °C, with the storage modulus (G'), loss modulus (G") and zero-point viscosity (η_0) recorded. Representative data were examined graphically to determine the linear viscoelastic region of the response to the applied stress, and to find the flow point when G' = G". The loss factor (tan δ) was calculated from G''/G' and the shear modulus (G*) from $\sqrt{(G'^2 + G''^2)}$.

Strain characterisation

Cell-surface adhesion (nN; pooled n = 50) was determined by Atomic force microscopy and force Spectroscopy (AFM-FS). Biofilm samples first drained of excess liquid for 30 min before being imaged in air at 20°C using a NanoWizard I Bio AFM Atomic Force microscope (JPK Instruments AG, Berlin, Germany). Samples were scanned in contact mode using silicon nitride triangular cantilevers, with a nominal spring constant of 0.01 N m^{-1}, scan speed of 0.5 µm s^{-1} and at resolutions of 100 x 100 µm down to 2.5 x 2.5 µm. In each sample, five cells were randomly selected, and cell-tip adhesion measured at ten different points along the exposed surface of each cell. Relative cell hydrophobicity (H_r; n = 5) was determined using a modification of the bacterial adherence to hydrocarbons (BATH) assay [35]. 1.2 ml of culture was washed three times in PBS (pH 7.2) and the cells re-suspended to an initial optical density (OD_{540}) of ~ 0.5. Samples were vortexed with 300 µl of n-hexadecane for 1 min and the phases allowed to separate for 30 min. The final OD_{540} was determined for the lower aqueous phase, and H_r calculated as 100 x ΔOD_{540} / initial OD_{540}. Maximum growth levels (OD_{600} 24 h^{-1}; n = 3) were determined in shaken and static microcosms after 24 h. Liquid surface tension (mN m^{-1}; n = 5) was determined for cell-free culture supernatants using a Krüss K100 Tensiometer (Krüss GmbH, Germany) at 20°C [17]; under these conditions the surface tension of deionised water and sterile KB-Fe was 72.4 ± 0.1 and 49.8 ± 0.2 mN m^{-1}, respectively. Recruitment to the surface (relative OD_{600}; n = 5) was measured after 2 h [13]. Cell

distributions (relative OD_{600}, *n* = 5) were also assessed in microcosms inoculated with a pellet of cells placed at the bottom of the vial, after 24 and 72 h, by sequentially sampling 1 ml aliquots from the top to the bottom [9]. Swimming motility (radius, cm; *n* = 3) on and through soft agar (0.1x KB nutrients, 1 µM $FeCl_3$ and 0.3 g L^{-1} agar) was assessed after 24 h. Colony expansion (radius, cm; *n* = 12) on standard KB-Fe plates containing 15 g L^{-1} agar was assessed after 24 h [12].

Competitive fitness and productivity

The competitive fitness (W) of CBFS, VM and WS were determined relative to the non-biofilm–forming SM-13 strain [18]. KB-Fe microcosms (*n* = 5) were inoculated with 100 µl of a 1:1 nominal mixture of strains (produced by adding equal volumes of over-night KB-Fe cultures) and incubated for 48 h under static or shaken conditions as required and these assays undertaken in batches for each level of disturbance. The fitness of one strain (A) competing against a second (B) was determined as the ratio of Malthusian parameters, $ln\ [A_{final} / A_{initial}] / ln\ [B_{final} / B_{initial}]$ [36], and cell numbers per microcosm were determined by enumeration of colonies on KB and KB-Kanamycin plates after vigorous mixing of microcosms, sampling and serial dilution. Fitness was also determined for pair-wise combinations of biofilm-types using 1000:1, 1:1 and 1:1000 nominal initial cell ratio mixtures (*n* = 5) under static incubation conditions for 72 h with all assays undertaken as a single batch. In these assays, trains differentiated by colony morphologies on KB plates, and actual strain ratios were determined from the initial cell numbers ($A_{initial} / B_{initial}$). Total final numbers ($A_{final} + B_{final}$) were also used to determine productivity (*n* = 5) in these microcosms.

Statistical analyses

Assays were performed with replicates (*n*) and means and standard errors (SE) are provided where appropriate. Data was analysed by JMP 12 (SAS Institute Inc, USA) and parametric or non-parametric approaches determined as required. Differences between means were determined using ANOVA models followed by *post hoc* Tukey-Kramer HSD tests or paired t-tests. Where appropriate the Wilcoxon (Rank Sums) tests were undertaken instead. Data were further investigated by correlation and linear regression (r^2). See **Supplementary Information S2** for further details of the statistical approach used here and for additional analyses reported in the Supplementary Information.

RESULTS AND DISCUSSION

CBFS, VM and WS biofilm-types are differentiable structures

The three biofilm-types studied here are readily distinguished by visual observation and we have classified them as physically cohesive (CBFS and WS) and viscous mass (VM)-class biofilms [16] (**Figure 1 (a)**). Our qualitative impressions of CBFS and WS robustness and VM fragility were confirmed by quantitative comparison of biofilm strength and attachment levels which clearly differentiates the three biofilms (T-K HSD, $\alpha = 0.05$; **Figure 1 (b)** and **Table 2 (a)**). We have extended our earlier rheological examination of VM biofilm samples [17] to include CBFS and WS samples (**Table 2 (b)**). This confirms that all three were viscoelastic structures as determined by loss factors ($\tan \delta$) of less than one, although other key rheological parameters differed significantly between biofilms (T-K HSD, $\alpha = 0.05$; Wilcoxon, $P \leq 0.05$; **Table 2 (b)**). Several other A-L interface biofilms, as well the VM biofilm produced by SBW25, have been examined *in situ* by interfacial rheology which also conclude that these are viscoelastic structures [37,38] as is the case for the more often studied liquid-solid surface (L-S) interface biofilms in which cells are similarly encased by a network of EPS fibres [39]. We interpret our results to suggest that the WS biofilm is the more resilient structure and is less brittle than the CBFS biofilm, and that both are stronger and better attached than the fragile VM biofilm.

Biofilm–formation also depends on a number of strain characteristics. These include swimming (and twitching) motility, relative cell hydrophobicity and cell adhesion, and the expression of surface active agents which are needed to approach, modify and successfully colonise a surface or interface. We observed significant differences in swimming in soft agar, with CBFS and WS cells apparently retarded by the over-expression of poly-acetyl glucosamine (CBFS), and cellulose and poly-acetyl glucosamine (WS), compared to VM cells (T-K HSD, $\alpha = 0.05$; **Table 2 (c)**) which presumably produce lower levels of these EPS or are not expressing them under these conditions. However, CBFS and VM cells swam at similar rates on the surface of soft agar which suggests the CBFS phenotype might change, perhaps in response to surface viscosity, other factors or interactions (the percentage of agar used in these assays is too low for swarming, although SBW25 is capable of this surface–associated motility [40]). Significant differences were also observed in recruitment rates to the top of the liquid column, relative cell hydrophobicity, and cell-surface adhesion, as well as in colony expansion which had previously been used to characterise the WS phenotype [12,41,42] (T-K HSD, $\alpha = 0.05$; **Table 2 (c)**) (we know that recruitment and adhesion of SBW25 and mutant cells are affected by EPS expression [9,13,43], and other studies suggest that large amounts of EPS may promote cell adhesion, e.g. [44]; a similar range of cell hydrophobicities are seen for other pseudomonads, e.g. [45], though H_r varies with the hydrocarbon tested [46]). However, no significant differences were seen in the surface tension of culture supernatants suggesting that all three expressed the surfactant viscosin [47], or in growth rates which suggests that they responded to O_2 levels in the same manner (T-K HSD, $\alpha = 0.05$; **Table 2 (c)**). However, it is notable that, across all three strains, a 1.4x higher growth level was achieved in shaken microcosms

with higher levels of aeration than static microcosms with more limited O_2 access (paired t-test, $P < 0.0001$).

Thirteen of 15 quantitative measurements we have made of biofilm strength and attachment levels, biofilm rheology and strain characteristics (**Table 2**) differentiate between CBFS, VM and WS biofilms. More similarities were found between CBFS and VM biofilms than with the WS biofilm, as determined by HCA (**Supplementary Figure S2**), which differs from our early qualitative grouping of these biofilms into physically cohesive and viscous mass-class biofilms [16] (**Figure 1 (a)**). Nonetheless, both the qualitative and quantitative assessments of biofilm phenotypes demonstrate that the CBFS, VM and WS biofilms can be differentiated by a number of characteristics and can be considered substantially different structures (quantitative biofilm phenotypes have not been reported for collections of WS or CBFS-like mutant isolates, e.g. in [10,14,15,48,49], so the range and overlap of biofilm-type phenotypes is unknown).

Our findings add to the growing number of reports demonstrating that naturally-occurring and engineered mutants are able to alter the physical characteristics of the biofilms produced by the wild-type strain, including KT2440, PA01 and PA14 which produce adaptive mutants similar to the Wrinkly Spreader in diversifying populations [27,28,29]. It would be interesting to know whether the variation in biofilm characteristics between wild-type and mutant strains is similar to the variation between wild-type biofilms grown under a range of environmental conditions, as this would impact on the fitness advantage biofilm mutants may have in diversifying populations and their ability to colonise new environments. Finally, as we have no reason to suppose that CBFS and VM-like biofilm mutants could not arise directly from wild-type SBW25 in one or two mutations, our physical comparison of these three proxy biofilm-types illustrates how adaptive radiation could result in multiple biofilm-based solutions to colonising the high-O_2 region of liquid columns through parallel or convergent evolution [50] (our use of the CBFS partially-engineered mutant and manipulation of wild-type SBW25 with exogenous Fe^{3+} were required as natural mutants with CBFS and VM biofilm phenotypes were not available).

Competitive fitness depends on the degree of physical disturbance

Although increased access to O_2 at the A-L interface underlies the fitness advantage of biofilm formation [5], these structures need to be sufficiently robust to withstand random physical disturbance yet still be cost-effective in terms of resource allocation for biofilm construction and growth. We therefor predict that as disturbance is increased, fitness should decline to the point where biofilm-formation provides no advantage or incurs a cost compared to non-biofilm–forming competitors. We tested competitive

fitness at four levels of disturbance, from standard static incubation conditions where disturbance is rare, low and intermediate levels of disturbance provided by a smooth-running orbital shaker, to high levels of disturbance provided by a more vigorous shaking incubator. Under low disturbance conditions, 48 h old CBFS and WS biofilms remained at the A-L interface but the VM biofilm sank within an hour, and under intermediate levels of disturbance all three biofilms sank within an hour.

Under static conditions the CBFS biofilm was found to provide the highest level of competitive fitness compared to the non-biofilm–forming reference strain SM-13 (W for CBFS, 2.7 ± 0.1) and significant differences in fitness were seen between all three strains (W for VM, 2.2 ± 0.1; WS, 1.8 ± 0.1; T-K HSD, α = 0.05). Furthermore, under these conditions each of the biofilm–forming strains can be considered adaptive lineages as fitness was greater than one (t-tests, $P < 0.05$), in agreement with earlier studies of VM and WS biofilms [11,32], and therefor are examples of convergent evolution (some prefer the term parallel evolution [48] but see [50]) (fitness or selection coefficients within WS and CBFS-like mutant isolates is known to vary e.g. [14,15,30,48,49], but as experimental conditions and reference strains differ, we cannot comment on the overlap of fitness ranges between biofilm-types). Our fitness assays also demonstrate that competitive fitness significantly declines with increasing levels of physical disturbance (T-K HSD, α = 0.05) (**Figure 2**) (in contrast, total productivity increases with disturbance, in agreement with our understanding that growth is O_2-limited in these microcosms; see **Supplementary Figure S3**). CBFS fitness fell the most, though only WS fitness was reduced to below one in the most vigorous shaking conditions (t-test, $P = 0.006$) (see **Supplementary Information S3** for further analysis of the fitness data confirming strain and disturbance effects).

These results clearly demonstrate that CBFS, VM and WS biofilm-forming lineages can out-compete a non-biofilm-forming competitor in static microcosms, but that as physical disturbance increases, the adaptive value of biofilm–formation rapidly falls in a strain and disturbance-dependent manner. In particular, we note that WS fitness did not change between static and low disturbance conditions, whereas CBFS and VM fitness significantly decreased (T-K HSD, α = 0.05) (**Figure 2**), supporting our earlier view that the WS biofilm was the more resilient structure and the VM biofilm the most fragile. We therefore conclude that the WS biofilm is better suited to the range of physical disturbance static microcosms are normally subject to than either the CBFS or VM biofilms.

Pair-wise competitions between CBFS, VM and WS

We undertook pair-wise competitive fitness assays with initial cell ratios of 1:1000, 1:1 and 1000:1 to determine which biofilm–former was likely to be successful if two mutants appeared at the same time in a radiating population, or if a second mutant appeared sometime after the first had become established

(three-way assays with two biofilm–forming strains plus SM-13 pose too many technical difficulties to be considered here). In these assays, both competitors are mixed uniformly throughout the liquid column and cells have to move into the high–O_2 region before they can form biofilms (similar assays have been undertaken before to determine relative fitness or selection coefficients within biofilm-types, e.g. [14,30,48,49]).

At or near the initial cell ratio of 1:1, the competitive fitness of CBFS and VM was significantly greater than WS fitness (**Figure 3**; T-K HSD, $\alpha = 0.05$), suggesting that these two strains can more rapidly colonise and dominate the A-L interface by forming biofilms than the WS under the conditions used here. However, across the range of initial cell ratios tested in these assays, fitness was found to be negative-frequency dependent for all pair-wise combinations and ranged between 0.52 ± 0.03 and 1.9 ± 0.1 for WS competing against VM when dominant and VM competing against WS when rare, respectively (**Figure 3**; a linear fit was found between the fitness of each strain and the log initial cell ratio, $r^2 = 0.77 – 0.98$; and fitness was also negatively correlated within strain pairs, $r^2 = -0.96 – -0.98$, $P < 0.0001$) (see **Supplementary Information S4** for further analysis of the fitness data confirming strain and ratio effects, and **Supplementary Figure S4** and **Supplementary Information S5** for an analysis of productivity that also confirms strain effects). We interpret these findings to mean that the fitness of CBFS, VM and WS biofilms is determined by strain characteristics and relative numbers, and to a lesser extent, on the identity of the competitor.

Negative frequency-dependent fitness arises as the proportions of competing strains change and within-strain competition for at least one limiting resource becomes more important than between-strain competition for the same resource (the suggestion that the increasing mass of the WS biofilm and likelihood of it sinking explains WS fitness decrease [3] does not apply to our model system, as in our two-day assays biofilms rarely sank). However, the reciprocal nature of the fitness within our pairwise biofilm competitions suggest that two limiting resources are needed to differentiate between the three strains. Although this will require further investigation, we suspect they are O_2 and nutrients; the presence of an extreme O_2 gradient within WS biofilms has already been established [6] and it is possible that a similar but inverted nutrient gradient is limiting growth at the very top layer of the biofilm (when nutrient levels are sufficiently low, O_2 is no longer growth-limiting and the WS fitness advantage is lost [8]; it would be intriguing to investigate cell distributions and fitness in microcosms containing nitrate or nitrite as alternative terminal electron acceptors, though we do not know whether SBW25 is capable of using these in anaerobic respiration). In the context of our model system, it is possible that multiple biofilm types may appear and co-exist for various lengths of time within the biofilm structure, where cell surface properties and EPS retain growing clonal populations and displace

competitors and diversity is maintained by multiple limiting resources allowing metabolic and growth trade-offs [2,3], even though the ready recognition of WS colonies on plates suggests that this is the most abundant and successful biofilm-type.

As substantial growth appears to occur in the liquid column below the VM biofilm compared to CBFS and WS biofilms (**Figure 1 (a)**), it is possible that some of the VM fitness advantage might be due to the colonisation of this region, as fitness is determined from total microcosm numbers rather than numbers from the biofilm itself. We confirmed that CBFS, VM and WS cell localisation throughout the liquid column varied with depth (T-K HSD, $\alpha = 0.05$; **Figure 4 (a-c)**) and between the three strains, with CBFS and WS having a higher proportion at the top than VM (Relative OD_{600} after 24 h, CBFS, 3.87 ± 0.11; WS, 3.55 ± 0.06; VM, 1.89 ± 0.03; T-K HSD, $\alpha = 0.05$; **Figure 4 (d)**) (enrichment at the top of the liquid column requires aerotaxis which has been demonstrated for both wild-type SBW25 and WS cells [9]). It is interesting to note that although the proportion of VM cells at the top did not significantly increase between 24 h and 72 hr, the proportion of WS cells increased (1.2x) as the WS biofilm became more visually obvious and the proportion of CBFS cells decreased (0.8x) as the liquid column below the CBFS biofilm became more turbid (T-K HSD, $\alpha = 0.05$; **Figure 4 (d)**). The proportion of VM cells located in the middle of the liquid column was significantly higher than CBFS and the proportion of WS cells the lowest (Relative OD_{600} after 24 h, CBFS, 0.60 ± 0.02; WS, 0.39 ± 0.02; VM, 0.78 ± 0.02; T-K HSD, $\alpha = 0.05$; **Figure 4 (e)**; see **Supplementary Information S6** for an analysis of cell distributions confirming strain and depth effects). These differences in cell localisation may reflect how CBFS, VM and WS biofilm structures develop over time and how efficiently each is able to retain their growing populations. However, localisation at the top does not require biofilm-formation per se, as wild-type SBW25 cells inhibited from forming a VM biofilm are also able to enrich in this region, though not as effectively as WS cells [9]. Nonetheless, the ability to colonise both the A-L interface by biofilm-formation and the rest of the liquid column with free-swimming cells might also reflect might reflect a trade-off between growth and competition, with cells near the A-L interface growing fast but subject to high levels of competition, and cells located further down the liquid column growing more slowly but with less competition.

CONCLUSIONS

Although biofilm research now has many established model systems, SBW25 is one of only a few bacteria reported to form a variety of A-L interface biofilms produced by adaptive mutants arising in diversifying populations or by genetic engineering. Our work has shown that the CBFS, VM and WS biofilms can be differentiated on the basis of physical structure, strain characteristics and fitness

advantage, allowing a link to be made between environmental conditions in which biofilms form, the structural resilience these must have in order to survive, and the fitness advantage they provide over other competitors. Although we have used the CBFS and VM biofilms here as proxies for naturally-occurring adaptive mutants which might arise in diversifying SBW25 populations as the Wrinkly Spreader did, our comparison of the three biofilm-types also illustrates how varied biofilm characteristics and fitness advantage might become between adaptive mutants arising from an ancestral biofilm–forming strain. It is possible that this variation may be greater than that seen between biofilms produced by the ancestor under different environmental conditions, and both variation in biofilm characteristics and the fitness advantage they provide may have significance in a range of medical, biotechnological and industrial contexts where the success of prophylactic treatments or continued productivity could be effected by unexpected diversity or change.

SUPPORTING INFORMATION AND DATA

Supporting information is available as a Supplementary Information file. *This will be made available from Mendeley Data on acceptance.*

AUTHOR STATEMENTS

ORCID Author identifiers: Robyn Jerdan, 0000-0002-7045-8362; Andrew Spiers, 0000-0003-0463-8629.
Roles undertaken by the Authors: Anna Koza: Design, experimentation and analysis; Robyn Jerdan: Design, experimentation, analysis and manuscript development; Scott Cameron: Manuscript development and supervision; Andrew Spiers: Design, experimentation, analysis, manuscript development and supervision. All authors contributed to the final manuscript preparation.

CONFLICTS OF INTERESTS

The authors declare that there are no conflicts of interests.

FUNDING INFORMATION

This work was partially funded by Abertay University (Scottish Charity Registration No: SC016040). Anna Koza's PhD studentship was funded by Abertay University while Robyn Jerdan's PhD studentship is self-funded.

ACKNOWLEDGMENTS

We thank Robert Jackson (University of Reading) and David Studholme (University of Exeter) for the sequencing of the CBFS2.1 genome, Paul Hallett (now at the University of Aberdeen) for help with the rheometry and Simon Hapca (now at the University of Stirling) for help with the initial statistical analyses. Andrew Spiers is a member of the Scottish Alliance for Geoscience Environment and Society (SAGES) and Anna Koza was a SAGES-associated PhD student.

REFERENCES

[1] **Flemming H-C, Wingender J, Szewzyk U, Steinberg P, Rice SA, Kjelleberg S.** Biofilms: an emergent form of bacterial life. *Nat Rev Microbiol* 2016;14:563–575.

[2] **Nadell CD, Drescher K, Foster KR.** Spatial structure, cooperation and competition in biofilms. *Nat Rev Microbiol* 2016;14:589–600.

[3] **Steenackers HP, Parijs I, Foster KR, Vanderleyden J.** Experimental evolution in biofilm populations. *FEMS Microbiol Rev* 2016;40:373–397.

[4] **Spiers AJ.** A mechanistic explanation linking adaptive mutation, niche change, and fitness advantage for the Wrinkly Spreader. *Int J Evolutionary Biol* 2014; Article ID 675432.

[5] **Koza A, Kuśmierska A, McLaughlin K, Moshynets O, Spiers AJ.** Adaptive radiation of *Pseudomonas fluorescens* SBW25 in experimental microcosms provides an understanding of the evolutionary ecology and molecular biology of A-L interface biofilm formation. *FEMS Microbiol Lett* 2017;364:fnx109.

[6] **Koza A, Moshynets O, Otten W, Spiers AJ.** Environmental modification and niche construction: developing O_2 gradients drive the evolution of the Wrinkly Spreader. *ISME J* 2011;5:665–673.

[7] **Yoder JB, Clancey E, Des Roches S, Eastman JM, Gentry L, Godsoe W, Hagey TJ, Jochimsen D, Oswald BP, Roberston J, Sarver BAJ, Schenks JJ, Spear SF, Harmon LJ.** Ecological opportunity and the origin of adaptive radiations. *J Evolutionary Biol* 2010;23:1581-1596.

[8] **Kuśmierska A, Spiers AJ.** New insights into the effects of several environmental parameters on the relative fitness of a numerically dominant class of evolved niche specialist. *Int J Evolutionary Biol* 2016;4846565.

[9] **Jerdan R, Kuśmierska A, Petric M, Spiers AJ.** Penetrating the air-liquid interface is the key to colonization and Wrinkly Spreader fitness. *Microbiology* 2019;165:1061–1074.

[10] **Rainey PB, Travisano T.** Adaptive radiation in a heterogeneous environment. *Nature* 1998;394:69–72.

[11] **Spiers AJ, Kahn SG, Travisano M, Bohannon J, Rainey PB.** Adaptive divergence in experimental populations of *Pseudomonas fluorescens*. I. Genetic and phenotypic bases of Wrinkly Spreader fitness. *Genetics* 2002;161:33–46.

[12] **Spiers AJ, Bohannon J, Gehrig S, Rainey PB.** Biofilm formation at the air–liquid interface by the *Pseudomonas fluorescens* SBW25 wrinkly spreader requires an acetylated form of cellulose. *Mol Microbiol* 2003;50:15–27.

[13] **Spiers AJ, Rainey PB.** The *Pseudomonas fluorescens* SBW25 wrinkly spreader biofilm requires attachment factor, cellulose fibre and LPS interactions to maintain strength and integrity. *Microbiology* 2005;151:2829–2839.

[14] **Bantinaki B, Kassen R, Knight CG, Robinson Z, Spiers AJ, Rainey PB.** Adaptive divergence in experimental populations of *Pseudomonas fluorescens*. III. Mutational origins of Wrinkly Spreader diversity. *Genetics* 2007;176:441–453.

[15] **Lind PA, Farr AD, Rainey PB.** Evolutionary convergence in experimental *Pseudomonas* populations. *ISME J* 2017;11:589–600.

[16] **Spiers AJ, Arnold DL, Moon CD, Timms-Wilson TM.** A survey of A-L biofilm formation and cellulose expression amongst soil and plant-associated *Pseudomonas* isolates. In: *Microbial Ecology of Aerial Plant Surfaces*. Bailey MJ, Lilley AK, Timms-Wilson TM (Eds). Wallingford: CABI; 2006. pp. 121–132.

[17] **Koza A, Hallett PD, Moon CD, Spiers AJ, 2009.** Characterisation of a novel air–liquid interface biofilm of *Pseudomonas fluorescens* SBW25. *Microbiology* 2009;155:1397–1406.

[18] **Green JH, Koza A, Moshynets O, Pajor R, Ritchie M., Spiers AJ.** Evolution in a test tube: rise of the Wrinkly Spreaders. *J Biological Educ* 2011;45:54—59.

[19] **Römling U, Galperin MY.** Bacterial cellulose biosynthesis: diversity of operons, subunits, products, and functions. *Trends Microbiol* 2015;23:545–557.

[20] **Remigi P, Ferguson GC, McConnell E, De Monte S, Rogers DW, Rainey PB.** Ribosome provisioning activates a bistable switch coupled to fast exit from stationary phase. *Mol Biol Evol* 2019;36:1056–1070.

[21] **Ude S, Arnold DL, Moon CD, Timms-Wilson T, Spiers AJ.** Biofilm formation and cellulose expression among diverse environmental *Pseudomonas* isolates. *Environ Microbiol* 2006;8:1997-2011.

[22] **Gjermansen M, Ragas P, Tolker-Nielsen T.** Proteins with GGDEF and EAL domains regulate *Pseudomonas putida* biofilm formation and dispersal. *FEMS Microbiol Lett* 2006;265:215–224.

[23] **Nielsen L, Li X, Halverson LJ.** Cell–cell and cell–surface interactions mediated by cellulose and a novel exopolysaccharide contribute to *Pseudomonas putida* biofilm formation and fitness under water-limiting conditions. *Environ Microbiol* 2011;13:1342–1356.

[24] **Robertson M, Hapca SM, Moshynets O, Spiers AJ.** Air-liquid interface biofilm formation by psychrotrophic pseudomonads recovered from spoilt meat. *Antonie van Leeuwenhoek* 2013;103:251–259.

[25] **Farias GA, Olmedilla A, Gallegos M-T.** Visualization and characterization of *Pseudomonas syringae* pv. tomato DC3000 pellicles. *Microbial Biotechnol* 2019;0:1–15.

[26] **Dragos A, Lakshmanan N, Martin M, Horvaath B, Maroti G, Garcia CF, Lieleg O, Kovacs AT.** Evolution of exploitative interactions during diversification in *Bacillus subtilis* biofilms. *FEMS Microbiol Ecol* 2018;94:fix155.

[27] **Boles BR, Thoendel M, Singh PK.** Self-generated diversity produces ‘‘insurance effects’’ in biofilm communities. *PNAS (USA)* 2004;101:16630–16635.

[28] **Flynn KM, Dowell G, Johnson TM, Koestler BJ, Waters CM, Cooper VS.** Evolution of ecological Diversity in Biofilms of *Pseudomonas aeruginosa* by altered cyclic diguanylate signalling. *J Bacteriol* 2016;198:2608–2618.

[29] **Bridier A, Piard JC, Bouchez T.** Emergence of a synergistic diversity as a Response to Competition in *Pseudomonas putida* biofilms. *Microb Ecol* 2019; 10.1007/s00248-019-01470-z.

[30] **Ferguson GC, Bertels F, Rainey PB.** Adaptive divergence in experimental populations of *Pseudomonas fluorescens*. V. Insight into the niche specialist Fuzzy Spreader compels revision of the model *Pseudomonas* radiation. *Genetics* 2013;195:1319–1335.

445 [31] **Gehrig SM.** Adaptation of *Pseudomonas fluorescens* SBW25 to the air-liquid interface: a study in
446 evolutionary genetics. DPhil Thesis. Oxford: University of Oxford; 2005.

447 [32] **Koza A.** Adaptation and niche construction by *Pseudomonas fluorescens* SBW25. DPhil Thesis.
448 Dundee: Abertay University; 2011.

449 [33] **Bailey MJ, Thompson IP.** Detection systems for phyllosphere Pseudomonads. In: *Genetic*
450 *Interactions Between Microorganisms in the Natural Environment.* Wellington EMR, van Elsas JD
451 (Eds). Oxford: Pergamon Press; 1992. pp. 127–141.

452 [34] **Rainey PB, Bailey MJ.** Physical and genetic map of the *Pseudomonas fluorescens* SBW25
453 chromosome. *Mol Microbiol* 1996;19:521–533.

454 [35] **Rosenberg M.** Bacterial adherence to hydrocarbons: a useful technique for studying cell surface
455 hydrophobicity. *FEMS Microbiol Lett* 1984;22:289-295.

456 [36] **Lenski RE, Rose M., Simpson SC, Tadler SC.** Long-term experimental evolution in *Escherichia coli.*
457 I. Adaptation and divergence during 2,000 generations. *Amer Nat* 1991;138:1315–1341.

458 [37] **Wu C, Lim JY, Fuller GG, Cegelski L.** Quantitative analysis of amyloid-integrated biofilms formed
459 by uropathogenic *Escherichia coli* at the air-liquid interface. *Biophys J* 2012;103:464-471.

460 [38] **Rühs PA, Böni L, Fuller GG, Inglis RF, Fischer P.** In-situ quantification of the interfacial rheological
461 response of bacterial biofilms to environmental stimuli. *PLoS ONE* 2013;8:e78524.

462 [39] **Peterson BW, He Y, Ren Y, Zerdoum A, Libera MR, Sharma PK, Van Winkelhoff A-J, Neut D,**
463 **Stoodleu P, Van der Mei H, Busscher HJ.** Viscoelasticity of biofilms and their recalcitrance to
464 mechanical and chemical challenges. *FEMS Microbiol Rev* 2015;39:234–245.

465 [40] **Alsohim AS, Taylor TB, Barrett GA, Gallie J, Zhang X-X, Altamirano-Junqueira AE, Johnson LJ,**
466 **Rainey PB, Jackson RW.** The biosurfactant viscosin produced by *Pseudomonas fluorescens* SBW25
467 aids spreading motility and plant growth promotion. *Environ Microbiol* 2014;16:2267–2281.

468 [41] **Spiers AJ.** Wrinkly-Spreader fitness in the two-dimensional agar plate microcosm: maladaptation,
469 compensation and ecological success. *PLoS ONE* 2007;2:e740.

470 [42] **Udall YC, Deeni Y, Hapca SM, Raikes D, Spiers AJ.** The evolution of biofilm–forming Wrinkly
471 Spreaders in static microcosms and drip-fed columns selects for subtle differences in wrinkleality
472 and fitness. *FEMS Microbiol Ecol* 2015;91;fiv057.

[43] **Fang HHP, Chan K-Y, Xu L-C.** Quantification of bacterial adhesion forces using atomic force microscopy (AFM). *J Microbiological Meth* 2000;40:89–97.

[44] **Tsuneda S, Aikawa H, Hayashi H, Yuasa A, Hirate A.** Extracellular polymeric substances responsible for bacterial adhesion onto solid surface. *FEMS Microbiol Lett* 2003;223:287–292.

[45] **Vanhaecke E, Remon J-P, Moors M, Raes F, De Rudder D, Van Peteghem A.** Kinetics of *Pseudomonas aeruginosa* adhesion to 304 and 316-L stainless steel: role of cell surface hydrophobicity. *Appl Envir Microbiol* 1990;56:788–795.

[46] **Stoimenova E, Vasileva-Tonkova E, Sotirova A, Galabova D, Lalchev Z.** Evaluation of different carbon sources for growth and biosurfactant production by *Pseudomonas fluorescens* isolated from wastewaters. *Z Naturforsch* 2009;64c:96–102.

[47] **de Bruijn I, de Kock MJ, Yang M, de Waard P, van Beek TA, Raaijmakers JM.** Genome-based discovery, structure prediction and functional analysis of cyclic lipopeptide antibiotics in *Pseudomonas* species. *Mol Microbiol* 2007;63:417–428.

[48] **McDonald MJ, Gehrig SM, Meintjes PL, Zhang X-X, Rainey PB.** Adaptive divergence in experimental populations of *Pseudomonas fluorescens*. IV. Genetic constraints guide evolutionary trajectories in a parallel adaptive radiation. *Genetics* 2009;183:1041–1053.

[49] **Lind PA, Farr AD, Rainey PB.** Experimental evolution reveals hidden diversity in evolutionary pathways. *eLife* 2015;4:e07074.

[50] **Arendt J, Reznick D.** Convergence and parallelism reconsidered: what have we learned about the genetics of adaptation? *Trends Ecol Evol* 2008;23:26–32.

FIGURE LEGENDS

Figure 1. The three biofilms produced by SBW25 have different phenotypes. Shown here are images of biofilms in situ and ex situ (**a**). Wild-type SBW25 (Ctrl) normally grows throughout the liquid column of static microcosms and does not produce a biofilm at the A-L interface or lumps of material when transferred to a Petri dish. In contrast, the CBFS and WS biofilms are robust-looking structures with a dry-looking top surface, are well-attached to the vial walls and produce large fragments when

transferred. The VM biofilm is a weak and poorly attached structure with a very wet-looking top surface and produces viscous strands of material when transferred. The control culture was grown in standard KB media and the CBFS, VM and WS biofilms in KB-Fe media. Microcosms were incubated for 72 h before testing. The three biofilms can be further differentiated by quantitative measurements of biofilm strength (g) and attachment levels (A_{570}) (**b**). Microcosms were incubated for 48 h before assay and means ± SE (n = 8) are shown. Means not connected by the same letter (normal text, strength; italics, attachment) are significantly different (T-K HSD, α = 0.05).

Figure 2. The fitness advantage of biofilm–formation is reduced as physical disturbance increases. Shown are the competitive fitness (W) of CBFS, VM and WS (**a – c**) relative to the non-biofilm–forming reference strain SM-13 in microcosms incubated with increasing degrees of physical disturbance (indicated by the triangles at the bottom of each graph), ranging from static (1) to vigorous shaking (4) conditions. When W > 1 the biofilm–forming strain has a competitive advantage over SM-13; when W < 1 SM-13 has the advantage. Microcosms were inoculated with a 1:1 ratio of the biofilm-forming strain and SM-13 and were incubated for 48 h before assay. Means ± SE (n = 5) are shown. Means not connected by the same letter within panels are significantly different (T-K HSD, α = 0.05). The grey background indicates W < 1. Dashed lines indicate trends only. Fitness under shaking conditions were further tested and means marked with an asterisk indicate where W ≠ 1 (t-test, $P \leq 0.05$).

Figure 3. Pairwise competitions between CBFS, VM and WS biofilms in static microcosms. Shown are the competitive fitness (W) of CBFS, VM and WS relative to one another in static microcosms inoculated with different initial strain ratios (**a – c**). When W > 1 the first strain has a competitive advantage over the second strain; when W < 1 the second strain has the advantage over the first strain. The small triangles indicate at what log ratio the strains are neutral (i.e. W = 1). Microcosms were inoculated with nominal 1:1000, 1:1 and 1:1000 cell ratios of the first and second strains, but data are shown here using the actual ratios determined from the initial cell number colony counts. Microcosms were incubated for 72 h before assay. Means ± SE (n = 5) are shown. Means not connected by the same letter within panels are significantly different (T-K HSD, α = 0.05). The grey background indicates W < 1. Dashed lines indicate trends only.

Figure 4. Cells distributions vary through the liquid column. Shown are the cell densities (relative OD_{600}) in samples (1 – 6) taken serially down the liquid column of static microcosms (**a – c**, CBFS, VM and WS), from the top and including any biofilm material (1) to the bottom (6). Cell densities in the top and middle samples (2 – 5) are compared on the right (**d & e**). Microcosms were inoculated with a cell pellet placed at the bottom of the vial and then incubated for 24 h (white circles) or 72 h (grey circles) before

assay. Means ± SE (n = 5) are shown. Means not connected by the same letter within panels are significantly different (T-K HSD, α = 0.05). The grey background indicates where relative densities are below one. Dashed lines indicate trends only.

TABLES

Table 1 : Biofilm-types produced by wild-type *P. fluorescens* SBW25 and mutants.

	Complementary Biofilm-forming Strain (CBFS)	Viscous Mass (VM)	Wrinkly Spreader (WS)
Strain origin	Diversifying population of the cellulose-deficient SBW25 *wssΔ* mutant	Wild-type strain	Diversifying population of wild-type SBW25
Genotype	SBW25 *wssΔ awsX* (CBFS2.1 [31])[a]	SBW25 (wild-type [33,34])	SBW25 *wspF* (archetypal strain [11,14])
Biofilm induction	Genetic (*awsX*), elevated c-*di*-GMP levels[b]	Physiological, exogeneous Fe^{3+}	Genetic (*wspF*), elevated c-*di*-GMP levels
Biofilm characteristics	Physically cohesive-class biofilm[c] Robust and well attached Dry-looking upper surface	Viscous mass-class biofilm[c] Fragile and poorly attached Wet-looking upper surface	Physically cohesive-class biofilm[c] Robust and well attached Dry-looking upper surface
Biofilm matrix / EPS	PGA[b]	Small amounts of cellulose, PGA	Higher levels of cellulose, PGA
Liquid column	Relatively little growth	More growth evident growth	Relatively little growth
Colony morphology	Intermediate, rough but rounded	Smooth and rounded	Flattened and wrinkled

a, See **Supplementary Information S1** for our identification of the likely biofilm-activating mutation in *awsX*. **b,** After similar mutants in which c-*di*-GMP and PGA were implicated by genetic means [15]. **c,** According to the classification of [16].

Table 2 : Quantitative differentiation of CBFS, VM and WS biofilms and strains.

		CBFS	VM	WS
(a) Biofilm measurements	Attachment (A_{570})	1.79 ± 0.03[a]	0.12 ± 0.01[c]	0.27 ± 0.02[b]
	Strength (g)	0.030 ± 0.002[b]	0.009 ± 0.003[c]	0.208 ± 0.005[a]
(b) Biofilm rheometry	Flow point (G' = G'') (Pa)	0.014 ± 0.001*	0.028 ± 0.004*	14 ± 2*
	Loss factor (tan δ)	0.52 ± 0.02[a]	0.46 ± 0.01[a]	0.28 ± 0.02[b]
	Shear modulus[†] (G*) (Pa)	0.27 ± 0.02*	0.8 ± 0.2*	130 ± 36*
	Zero shear viscosity (η_0) (Pa s)	0.087 ± 0.005*	0.24 ± 0.05*	41 ± 11*
(c) Strain characteristics	Cell hydrophobicity (H_r)	0.44 ± 0.02[a]	0.19 ± 0.02[b]	0.08 ± 0.03[c]
	Cell-surface adhesion (nN)	-13.2 ± 0.1[b]	-12.1 ± 0.1[a]	-15.2 ± 0.2[c]
	Colony expansion (cm 24 h^{-1})	0.38 ± 0.01[b]	0.40 ± 0.01[b]	0.75 ± 0.02[a]
	Growth in shaken microcosms (OD_{600} 24 h^{-1})	1.39 ± 0.04[a]	1.38 ± 0.02[a]	1.38 ± 0.03[a]
	Growth in static microcosms (OD_{600} 24 h^{-1})	1.00 ± 0.01[ab]	1.01 ± 0.03[a]	0.91 ± 0.02[b]
	Liquid surface tension (mN m^{-1})	25.6 ± 0.2[a]	25.2 ± 0.2[a]	25.8 ± 0.1[a]
	Recruitment (relative OD_{600})	0.70 ± 0.02[b]	0.77 ± 0.01[a]	0.80 ± 0.02[a]
	Swimming in soft agar (cm 24 h^{-1})	0.28 ± 0.03[b]	0.93 ± 0.07[a]	0.35 ± 0.08[b]
	Swimming on soft agar (cm 24 h^{-1})	1.2 ± 0.05[a]	1.08 ± 0.08[a]	0.53 ± 0.06[b]

Means ± SE are shown. Means not connected by the same letter are significantly different (T-K HSD, $\alpha = 0.05$), and where appropriate, * indicates where all pairwise combinations are significantly different (Wilcoxon, $P \leq 0.05$). [†], Also known as the modulus of rigidity and sometimes denoted by S or μ. Biofilm rheometry for the VM biofilm was originally presented in [17].

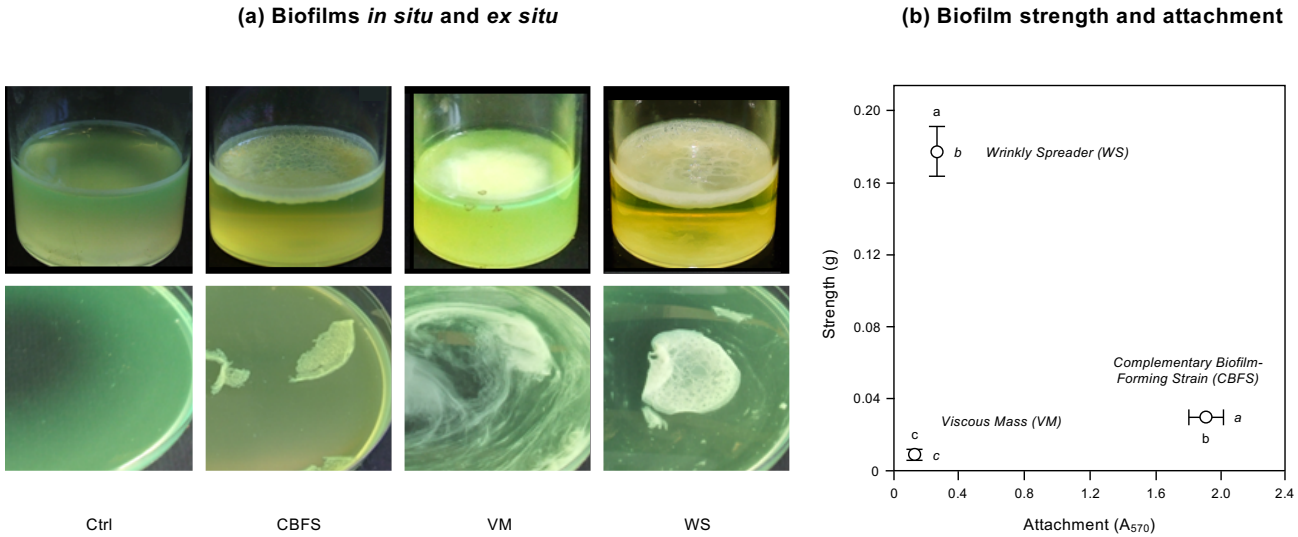
(a) Biofilms *in situ* and *ex situ*
(b) Biofilm strength and attachment
Ctrl
CBFS
VM
WS
Strength (g)
Attachment (A_{570})
0
0.04
0.08
0.12
0.16
0.20
0.4
0.8
1.2
1.6
2.0
2.4
a
b
Wrinkly Spreader (WS)
Complementary Biofilm-Forming Strain (CBFS)
Viscous Mass (VM)
c

Figure 1

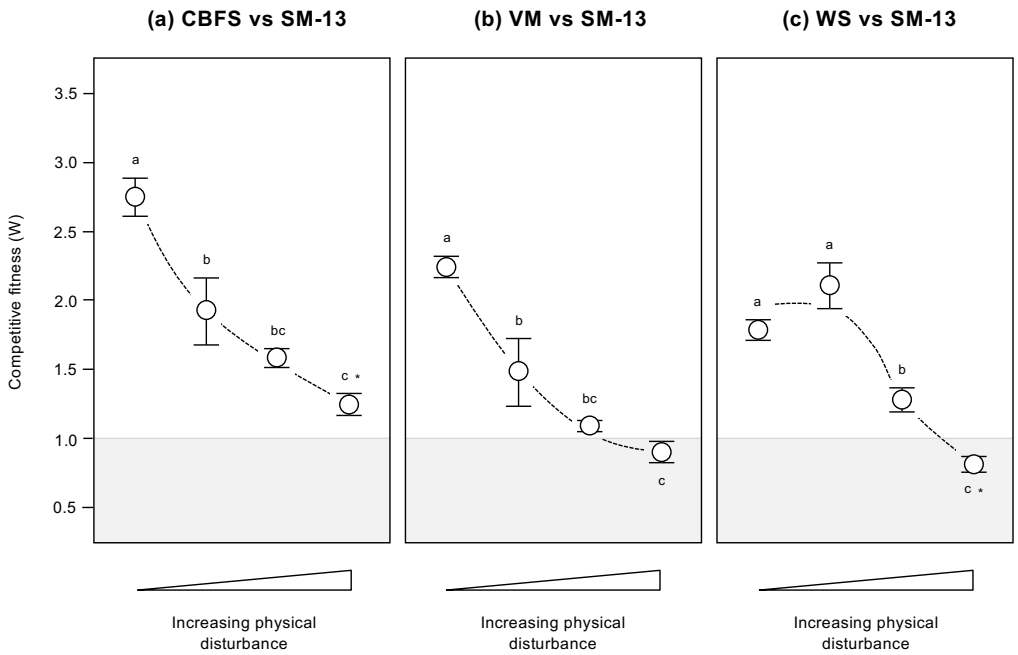
(a) CBFS vs SM-13
(b) VM vs SM-13
(c) WS vs SM-13
Competitive fitness (W)
3.5
3.0
2.5
2.0
1.5
1.0
0.5
a
b
bc
c *
a
b
bc
c
a
a
b
c *
Increasing physical disturbance
Increasing physical disturbance
Increasing physical disturbance

Figure 2

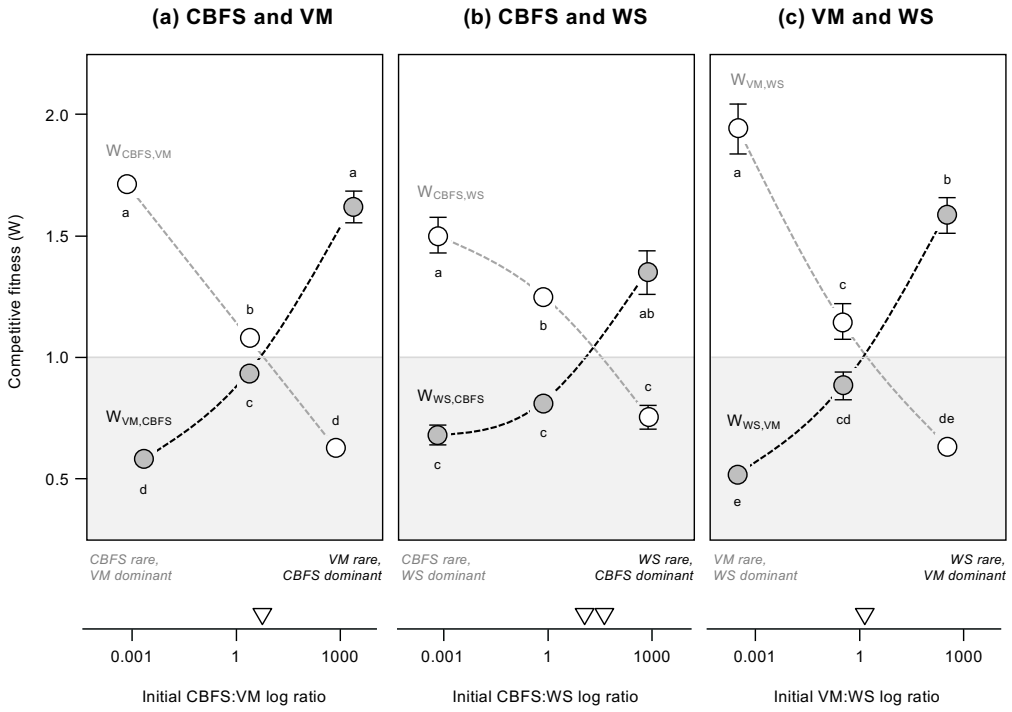
(a) CBFS and VM
(b) CBFS and WS
(c) VM and WS
Competitive fitness (W)
2.0
1.5
1.0
0.5
W_CBFS,VM
W_VM,CBFS
W_CBFS,WS
W_WS,CBFS
W_VM,WS
W_WS,VM
a
b
c
d
ab
cd
de
e
CBFS rare, VM dominant
VM rare, CBFS dominant
CBFS rare, WS dominant
WS rare, CBFS dominant
VM rare, WS dominant
WS rare, VM dominant
0.001
1
1000
Initial CBFS:VM log ratio
Initial CBFS:WS log ratio
Initial VM:WS log ratio

Figure 3

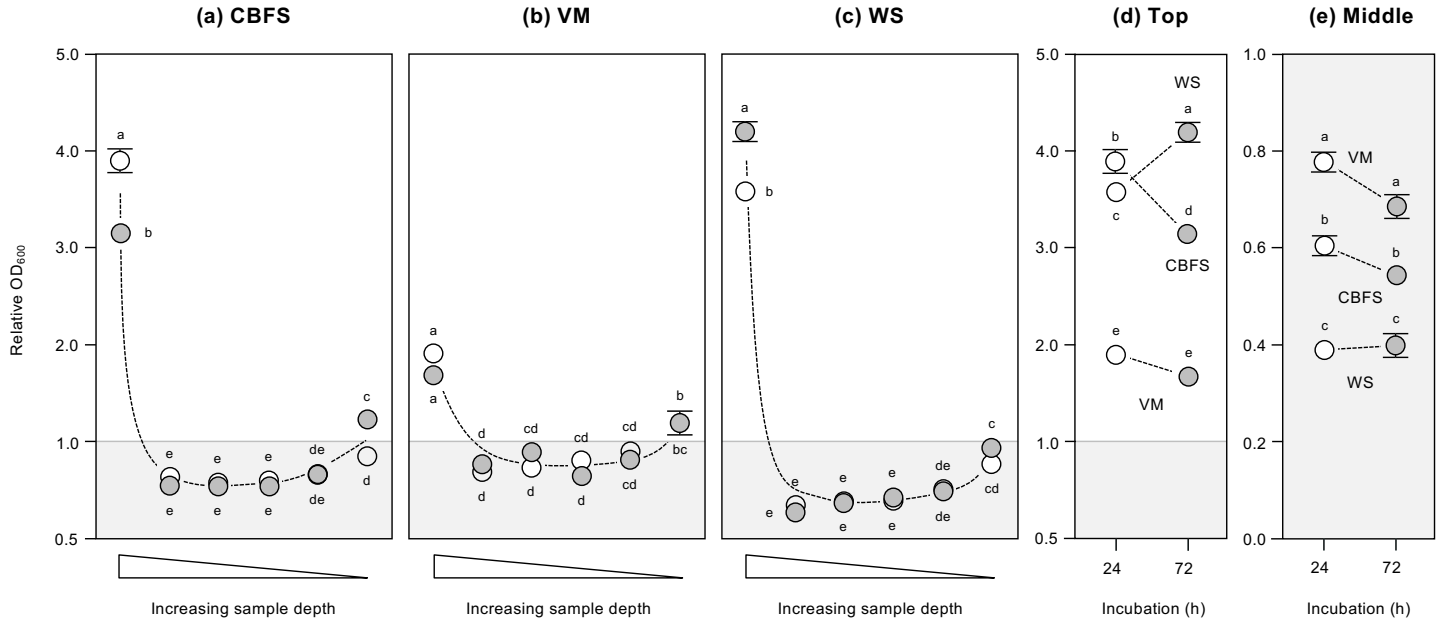
(a) CBFS
(b) VM
(c) WS
(d) Top
(e) Middle
Relative OD600
Increasing sample depth
Increasing sample depth
Increasing sample depth
Incubation (h)
Incubation (h)
24
72
WS
CBFS
VM
VM
CBFS
WS

Figure 4

SUPPLEMENTARY INFORMATION

Three biofilm types produced by a model pseudomonad are differentiated by structural characteristics and fitness advantage

Anna Koza, Robyn Jerdan, Scott Cameron, and Andrew J. Spiers

SUPPLEMENTARY INFORMATION SECTIONS S1 – S6

S1: Identification of the *awsX* mutation in CBFS2.1

CBFS2.1 was an unknown biofilm-forming mutant isolated from a diversifying population of the cellulose-deficient SBW25 strain, SBW25 Δ*wss* [1]. We determined the genome sequence of CBFS2.1 with the help of Robert Jackson (University of Reading) and David Studholme (University of Exeter) in which a mutation in *awsX* (PFLU5211) was identified involving the deletion of 11 amino acids (YTDDLIKGTTQ). AwsX is a regulator of the diguanylate cyclase (DGC) AwsR, and mutations in *awsX* in a wild-type SBW25 background result in the WS phenotype [2] through increased c-*di*-GMP levels and activation of the cellulose synthase complex. However, *awsX* mutations in a SBW25 Δ*wss* background result in the over-expression of PGA instead (these are collectively known as the PWS mutants [3]). For this reason, we suggest that CBFS2.1 is similar to the PWS mutants and also expresses PGA to produce an A-L interface biofilm.

S1 References

[1] **Gehrig SM.** Adaptation of Pseudomonas fluorescens SBW25 to the air-liquid interface: a study in evolutionary genetics. DPhil Thesis. Oxford: University of Oxford; 2005..

[2] **McDonald MJ, Gehrig SM, Meintjes PL, Zhang X-X, Rainey PB.** Adaptive divergence in experimental populations of *Pseudomonas fluorescens*. IV. Genetic constraints guide evolutionary trajectories in a parallel adaptive radiation. *Genetics* 2009;183:1041–1053.

[3] **Lind PA, Farr AD, Rainey PB.** Evolutionary convergence in experimental *Pseudomonas* populations. *ISME J* 2017;11:589–600.

S2: Statistical analyses

Assays were performed with replicates (*n*) as a single batch unless otherwise indicated and means and standard errors (SE) are provided where appropriate. Data was analysed by JMP 12 (SAS Institute Inc, USA) using a parametric approach having first determined that the data or residuals had a Normal distribution. Where necessary, outlier analysis was used and data progressively removed until a Normal distribution was achieved, as determined by fitting a Normal distribution and using the Shapiro-Wilk W Test ($P > 0.05$) to check the goodness of fit. Differences between means were determined using ANOVA models followed by *post hoc* Tukey-Kramer HSD tests. Where necessary, a nonparametric comparison using the Wilcoxon method was employed instead. A paired t-test was used to investigate differences in growth in shaken and static microcosms, and further t-tests used to determine if competitive fitness was equal to one. Similarities between biofilms was investigated by Hierarchical cluster analysis (HCA) using the Ward method with ordinal values derived from the biofilm structure, rheology and strain characterisation data. General linear (mixed) modelling (GLM/GLMM with Summary of fit, RSquare) approaches with standard least squares personalities were used to model competitive fitness and productivity with *post hoc* differences between means determined using LSMeans Differences Student's t and Tukey HSD tests. Correlations between data were examined (r^2) and fits between fitness as the response and log [initial cell ratio] as the regressor were determined by linear regression.

S3: Further analysis of competitive fitness across a range of physical disturbance levels

Competitive fitness was modelled using a GLM approach with strain (CBFS, VM, WS; character, nominal), disturbance (four levels from static (1) to shaken (4); character, ordinal) and replicate (character, nominal) effects, and a strain x disturbance interaction effect (GLM summary statistics: RSquare = 0.89; ANOVA, $F_{15,40} = 21.85$, $P < 0.0001$). This found significant strain, disturbance and strain x disturbance interaction effects ($P < 0.0001$, < 0.0001 and 0.0003), but no replicate effect ($P = 0.53$). Both strain and disturbance levels could be further differentiated, with CBFS having the highest over-all fitness of 1.85 across the range of disturbances, followed by WS (1.45) and then VM (1.41), and the static incubation conditions producing the highest fitness of 2.24 across the strains and the shaking incubation producing the lowest fitness of 0.97 as expected (LSMeans Differences T-HSD, $\alpha = 0.05$).

S4: Further analysis of competitive fitness from the pairwise competitions

Competitive fitness was first modelled using a GLMM approach for each pairwise competition, with first strain (CBFS, VM, WS; character, nominal), ratio (log of the actual initial cell ratio, calculated for the first strain) (numeric, continuous), and replicate effects and a first strain x ratio interaction effect. In the CBFS and VM competitions (GLMM summary statistics: RSquare = 0.98; ANOVA, $F_{7,17} = 150.03$, $P < 0.0001$), first strain, ratio and first strain x ratio interaction effects ($P < 0.0001$, 0.02 and < 0.0001) were found, but no replicate effect ($P = 0.96$). However, no significant correlation was found between the pooled fitness and log ratio ($P = 0.41$). In the CBFS and WS competitions (GLMM summary statistics: RSquare = 0.88; ANOVA, $F_{7,21} = 21.11$, $P < 0.0001$), significant first strain and first strain x ratio interaction effects ($P < 0.0001$) were found, but no ratio or replicate effects ($P = 0.19$ and 0.99). No correlation was found between the pooled fitness and log ratio ($P = 0.5$). Finally, in the VM and WS competitions (GLMM summary statistics: RSquare = 0.97; ANOVA, $F_{7,15} = 65.88$, $P < 0.0001$), significant first strain and first strain x ratio interaction ($P = 0.004$ and < 0.0001) effects and a weak ratio effect ($P = 0.06$) were found, but no replicate effect ($P = 0.48$). However, no significant correlation was found between the pooled fitness and log ratio ($P = 0.75$). In all three models, both strains could be differentiated from one another (LSMeans Differences Student's t, $\alpha = 0.05$). These confirm that strain fitness is differentiated within pairwise assays, and that fitness is dependent on the initial cell ratios.

Competitive fitness was also modelled using a GLMM approach for all pairwise competitions, with first strain, strain pair (CBFS & VM, CBFS & WS, VM & WS; character, nominal), ratio and replicate (character, nominal) effects (GLMM summary statistics: RSquare = 0.91; ANOVA, $F_{9,67} = 74.96$, $P < 0.0001$). This found significant first strain, strain pair and ratio effects ($P < 0.0001$, 0.005 and 0.0001) effects, but no replicate effect ($P = 0.95$). However, no significant correlation was found between the pooled fitness and log ratio ($P = 0.49$). This confirms the effect findings from the individual models and in addition shows that there are significant differences in fitness between each of the strain combinations tested in these pairwise assays.

S5: Further analysis of productivity from the pairwise competitions

Productivity was modelled using a GLMM approach with strains (CBFS & VM, CBFS & WS, VM & WS; character, nominal), ratio (log of the actual initial cell ratio, calculated for the first strain) (numeric, continuous), and replicate effects (GLMM summary statistics: RSquare = 0.36; ANOVA, $F_{7,37} = 2.96$, $P = 0.01$). This found a significant strain effect ($P = 0.003$) and a weak ratio effect ($P = 0.07$), but no replicate effect (0.78). A weak correlation was also found between the pooled productivity and log ratio ($r^2 = 0.30$ $P = 0.4$). This confirms that productivity is affected by the strain combinations and initial cell ratios.

S6: Further analysis of cell distributions

Cell distributions were modelled using a GLM approach separately for the 24 and 72 h incubation experiments as a Normal distribution of residuals was not readily achieved for the combined data. For both experiments, cell distributions were modelled with strain (CBFS, VM, WS, character, nominal), depth (1 – 6, numeric, ordinal) and replicate (character, nominal)

effects (GLM summary statistics for the 24 h experiment: RSquare = 0.99; ANOVA, $F_{11,64}$ = 491.51, P < 0.0001; 48 h experiment: RSquare = 0.99; ANOVA, $F_{11,56}$ = 413.81, P < 0.0001). This found significant strain and depth effects (24 and 72 h, P < 0.0001) but no replicate effects (24 h, P = 0.24; 72 h, P = 0.40). In both experiments, CBFS, VM and WS could be differentiated from one another (LSMeans Differences T-HSD, α = 0.05), and the top (1), middle-depth samples (2 – 5) and bottom (6) samples from one another (LSMeans Differences T-HSD, α = 0.05).

SUPPLEMENTARY INFORMATION FIGURES S1 – S4

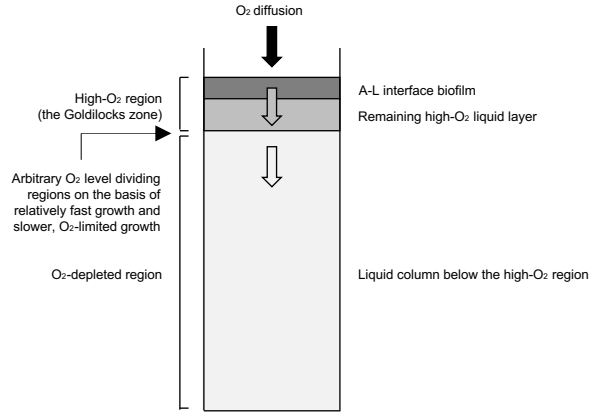

Figure S1. The static microcosm is divided into different regions. The metabolic activity of the initial SBW25 colonists randomly distributed through the liquid column rapidly establishes an O_2 gradient and divides the microcosm into a shallow high-O_2 region and a deeper O_2-depleted region. An air-liquid (A-L) interface biofilm can be formed at the liquid surface of the high-O_2 region, and both this and the remaining high-O_2 layer below it are also known as the Goldilocks zone. However, as the biofilm develops and deepens, O_2 flux through the biofilm is further reduced and the high-O_2 liquid layer becomes shallower (ultimately the division between high-O_2 and depleted-O_2 regions moves up into the biofilm).

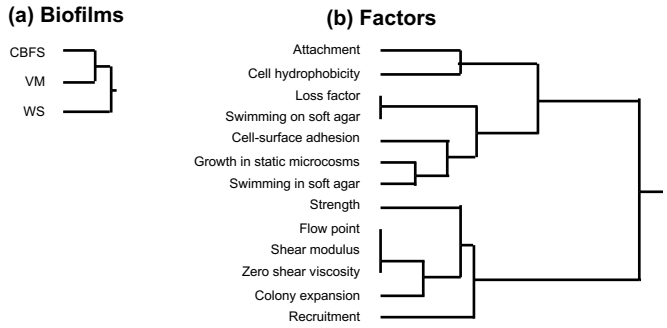

Figure S2. Biofilms are differentiated by a range of quantifiable factors. Shown are the results of a two-way Hierarchical cluster analysis (HCA) using biofilm structure, rheology and strain characterisation data (n = 13). Biofilms are clustered according to similarity in (**a**) and factors according to similarity in (**b**).

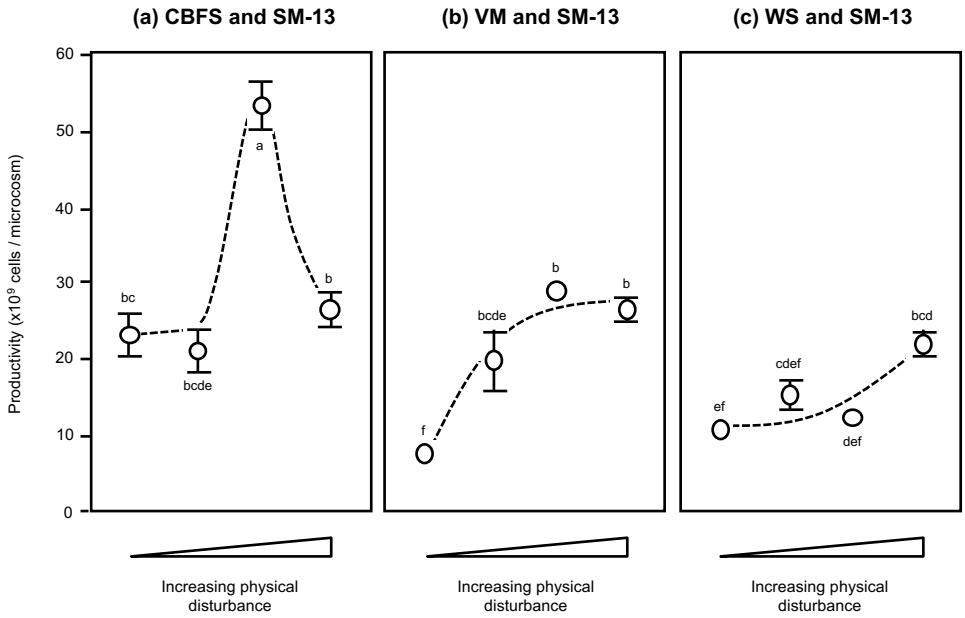

Figure S3. Productivity in the physical disturbance assays. Shown are the productivities determined as the total final cell numbers (**a – c**, CBFS, VM or WS plus SM-13) per microcosm for the competitive fitness assays which were incubated with increasing degrees of physical disturbance (indicated by the triangles at the bottom of each graph), ranging from static (1) to vigorous shaking (4) conditions. Means ± SE (n = 5) are shown. Means not connected by the same letter within and across panels are significantly different (T-K HSD, α = 0.05). Dashed lines indicate trends only.

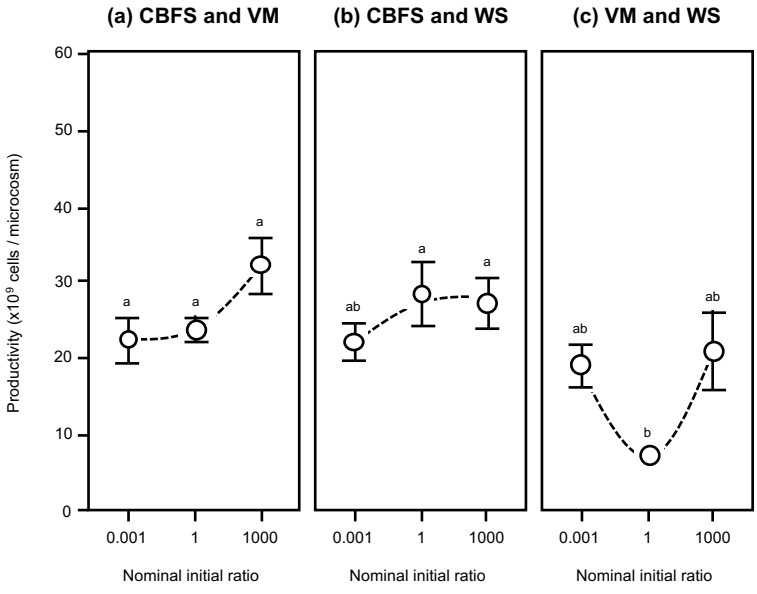

Figure S4. Productivity in the pairwise competition assays. Shown are the productivities determined as the total final cell numbers (**a – c**, CBFS and VM, CBFS and WS, and VM and WS) per microcosm for the competitive fitness assays with nominal initial cell ratios of 0.001, 1 and 1000. Means ± SE (n = 5) are shown. Means not connected by the same letter within and across panels are significantly different (T-K HSD, α = 0.05). Dashed lines indicate trends only.